

## UNSTEADY LAMINAR FLOW AND HEAT TRANSFER IN A ROTATING CAVITY WITH A STATIONARY OUTER SURFACE

T. W. Lewis, M. Wilson and D. A. S. Rees

Department of Mechanical Engineering  
University of Bath  
Bath BA2 7AY  
United Kingdom

### ABSTRACT

This paper describes the computation of laminar flow and heat transfer in a rotating cavity with a stationary outer surface, using time-dependent, axisymmetric numerical simulations. The geometric configuration is based on a cavity formed by co-rotating turbine discs in a gas-turbine engine. Unsteady flow computations are carried out for a rotational Reynolds number (based on the outer radius of the disc) of  $10^4$ , with one hot disc and one cold disc. For incompressible flow, a periodic unsteady flow develops, while for computations including variable density effects (through the Boussinesq approximation) the flow reaches a steady-state for some values of Rayleigh number. The computed Nusselt number distribution for the hot disc is significantly affected by unsteady flow and variable density effects. Some of these findings also apply to computations carried out at a higher rotational Reynolds number.

### 1 INTRODUCTION

Fig. 1 illustrates the rotating cavity studied in this paper. The system comprises two corotating discs, one heated and one unheated, a rotating inner surface and a stationary outer surface. These two cylindrical surfaces are both adiabatic. The aspect ratio of the cavity is given by  $G (= s/b) = 0.3$ . Gan et al (1996) made measurements and carried out steady-state, axisymmetric computations for the turbulent flow in such a system under isothermal conditions. The configuration was used as a model for the rotating cavity formed by co-rotating turbine discs in a gas-turbine engine. Mirzaee et al (1996) studied heat transfer for this system with the addition of a superposed flow of air. The flow and heat transfer in rotating cavities, and applications to air-cooling inside

gas turbines, are described in detail by Owen and Rogers (1995).

Fig. 1 also illustrates the twin, symmetric secondary flow recirculations computed by Wilson et al (1997) for rotational Reynolds number  $Re_\phi = 10^4$ , under assumptions of steady, axisymmetric laminar flow. There is radial outflow in boundary layers on the two discs, and a radial inflow is formed where the boundary layers meet along the stationary outer surface. Gan et al (1996) obtained similar results for steady turbulent flow at higher rotational Reynolds numbers, and these computed flow structures were supported by measurements of velocity distributions made using laser Doppler anemometry. The penetration of the recirculating flow radially inward decreased with increasing  $Re_\phi$ .

There were a number of simplifications and uncertainties in the work on this cavity described Gan et al (1996) and Mirzaee et al (1997), some of which contributed to the incomplete agreement obtained between the measurements of turbulent flow and heat transfer and the axisymmetric, steady computations. First, an isotropic  $k-\epsilon$  turbulence model (Launder and Sharma, 1974) was used to close the Reynolds-averaged Navier-Stokes equations, and this was not able to predict accurately the combined free and forced (or Rankine) vortex flow which measurements showed to develop. Also, for heat transfer cases (which involved 3D flow from discrete inlet nozzles in the experiment), the surface temperature of the heated disc was measured but the temperature of the other (unheated) disc was not, and semi-empirical conduction assumptions were made for this disc which had a significant effect on computed heat transfer results. Finally, incompressible flow was assumed.

Wilson et al (1997), motivated by convergence difficulties encountered in the steady flow computations

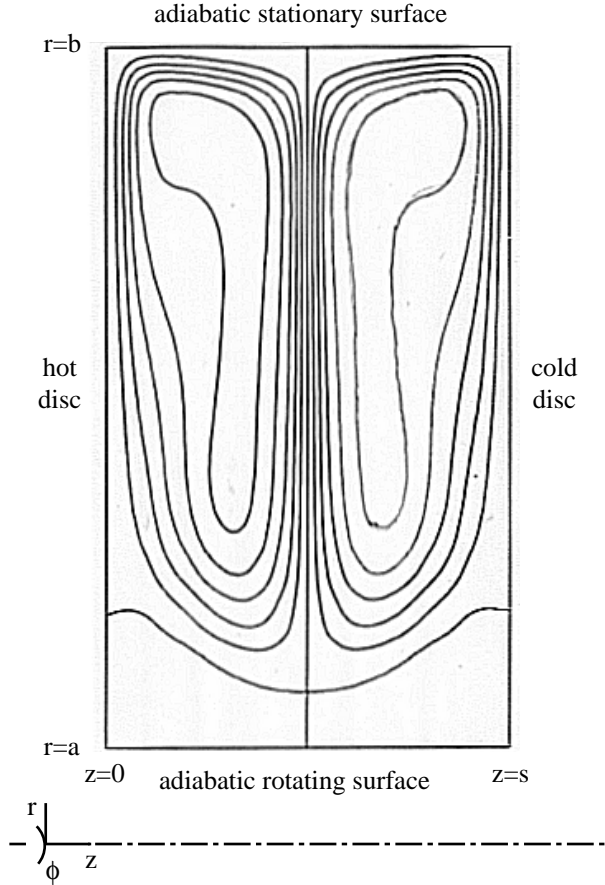


Fig. 1 The rotating cavity, and computed secondary flow streamlines, for steady incompressible flow at  $Re_\phi = 10^4$

reported by Gan et al, carried out *time-dependent* axisymmetric computations for the "closed" rotating cavity (i.e. without a superposed flow), at the lowest rotational speed for which experimental flow data were available (corresponding to  $Re_\phi = 1.46 \times 10^5$ ). It was found that unsteady flow developed which was not periodic. This unsteady solution gave rise to a time-averaged tangential velocity distribution showing Rankine vortex behaviour, and in better agreement with measurements than was obtained for a steady flow solution.

This paper describes computations of unsteady, axisymmetric, laminar flow and heat transfer for the closed cavity shown in Fig. 1, for which the computed effects of unsteadiness can be studied without the difficulties in matching experimental conditions referred to above. It is expected that the laminar flow results described here will inform future, improved computations of turbulent flow cases for which measured data exist.

The computational procedure is described in section 2. Flow and heat transfer results for incompressible flow calculations are discussed in section 3, and the effects of density variations are considered in section 4. Conclusions and recommendations for future work are given in section 5.

## 2 COMPUTATIONAL METHOD

Numerical simulations were carried out using the axisymmetric time-dependent solver for the streamfunction-vorticity form of Navier-Stokes equations described by Wilson et al (1997), and including solution of the energy equation. The time-dependent vorticity and tangential velocity equations were solved explicitly in a rotating frame of reference using the Du-Fort Frankel method. The solution time-step was determined from numerical stability studies for each different calculation.

A fixed V-cycle multigrid algorithm with line-relaxation smoothing was used in solving the Poisson equation for the streamfunction. Multigrid convergence at each time-step required the total absolute residual on the mesh to fall below  $10^{-6}$  for the Poisson equation solution (for which the maximum streamfunction value was around 50). Values of vorticity on the boundaries were updated using the streamfunction solution at the new time level.

Solutions were obtained on a collocated finite-difference grid, contracted to the solid surfaces and equi-spaced (separately in the axial and radial directions) in the centre of the domain. Hybrid-upwind differencing was used for the non-linear convection terms, and a first-order-accurate forward difference in time was employed. Further details of the grid, and the results of grid-dependence tests, are given in subsequent sections.

The fluid was initially at rest in the stationary frame of reference, and the rotating surfaces assumed a fixed given speed instantaneously at time  $t = 0$ . In order to perturb the solution from a symmetric twin recirculation structure (Fig. 1), a small axially varying perturbation to the tangential velocity could be introduced. It was found, however, that amplification of round-off errors in the solution was sufficient to perturb the flow, and the results presented here do not include the use of an imposed perturbation.

The time-dependent energy equation was solved in the same way as those for the vorticity and tangential velocity. The fluid was initially at the same temperature as the isothermal cold disc,  $T_s = 308$  K, and the hot disc was given a higher uniform temperature  $T_0$  at time zero. The disc temperatures considered were loosely based on those given by Mirzaee et al (1997) for systems involving a superposed cooling flow (heat transfer studies were not conducted for the closed cavity). The cold disc temperature  $T_s$  was used in this work to calculate reference values of fluid properties.

For variable density calculations the Boussinesq approximation was introduced, in which the density is assumed to be linearly dependent on temperature but independent of pressure, i.e.

$$\rho = \rho_0 [ 1 - \beta(T - T_s) ] \quad (1)$$

where  $\rho_0$  is a reference density and  $\beta$  is the volumetric

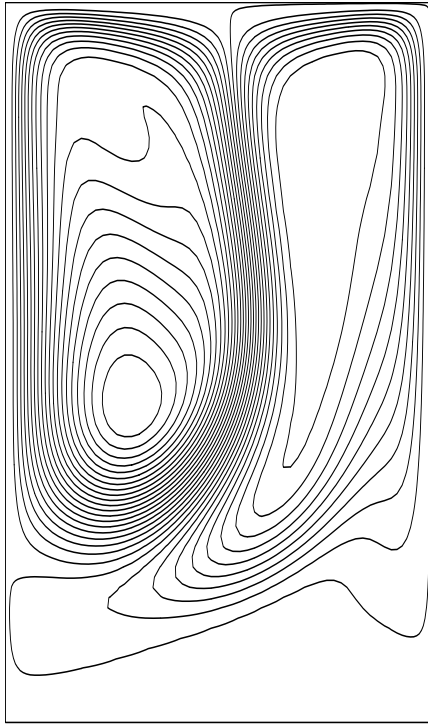


Fig. 2 Instantaneous secondary flow streamlines for unsteady incompressible flow computation:  $Re_\phi = 10^4$

expansion coefficient. It is assumed that this approximation is negligible in all but the Coriolis and centrifugal terms, i.e. the fluid is a Boussinesq fluid. To preserve the validity of this approximation, the largest temperature difference considered was  $\Delta T (= T_o - T_s) = 100$  K. As buoyancy effects introduce asymmetry into the flow, no other initial perturbation to the flow would be required for these calculations.

### 3 CONSTANT DENSITY FLOW RESULTS

Fig. 2 shows instantaneous computed streamlines for unsteady laminar flow at  $Re_\phi = 10^4$ , with  $\Delta T = 50$  K.

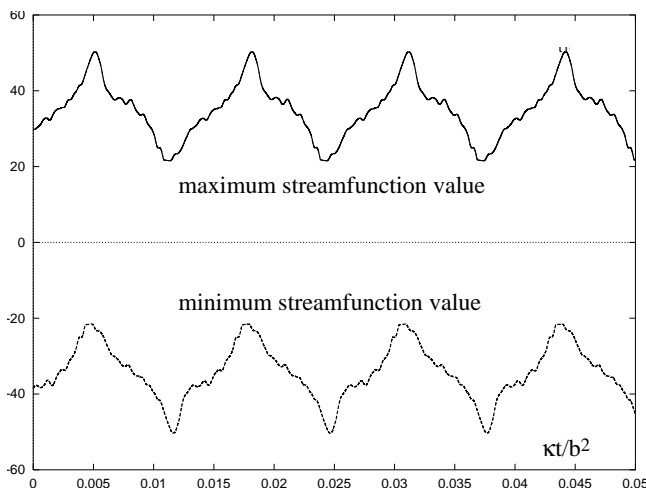


Fig. 3 Streamfunction time-history for unsteady incompressible flow computation:  $Re_\phi = 10^4$

The nondimensional time-step ( $\kappa\delta t/b^2$ ) was  $10^{-6}$ , and an  $80 \times 96$  axial by radial grid was used. The computed flow was periodic, as illustrated in Fig. 3 by the variation with time of the maximum and minimum value of the streamfunction. These extrema occur at the centre of the two recirculations established about the axial mid-plane of the cavity ( $z/s = 1/2$ ). The periodic variation is between the structure shown in Fig. 2, where the stronger recirculation is nearer the heated disc and the radial inflow moves toward the hot disc in the inner part of the cavity, and the equal but opposite situation where the stronger recirculation is closer to the cold disc. (The secondary peaks seen in these streamfunction variations were found to reduce when smaller time steps were used, however the other features of the solution were not affected).

Fig. 4 shows the effect of the unsteadiness in the flow on the heat transfer from the hot disc. The standard deviation of local Nusselt number,  $Nu$ , about the time-averaged radial distribution is shown (the abscissa  $x = r/b$  is the nondimensional radius on the disc). The Nusselt number distribution resulting from a steady-state calculation is also shown in Fig. 4, and is in poor agreement with the distributions obtained for unsteady flow. The steady solution was obtained by solving the half-problem for the cavity, with symmetry conditions imposed for the flow at the axial mid-plane, and with the mid-plane fluid temperature set to  $T_s + \Delta T/2$ . The solution, and the computed steady-state  $Nu$  distribution shown in Fig. 4, was very close to that obtained by solving the full problem with the steady-state finite-volume solver used by Mirzaee et al (1997), and with which the symmetric secondary flow prediction shown in Fig. 1 was obtained.

The steady-state distribution shown in Fig. 4 has a peak value for  $Nu$  at  $x \approx 0.65$ , which is close to the innermost point of the recirculations shown in Fig. 1. For the time-averaged distribution, the peak value for  $Nu$  is further radially outward at  $x \approx 0.75$ , and increased activity in the unsteady flow leads to higher

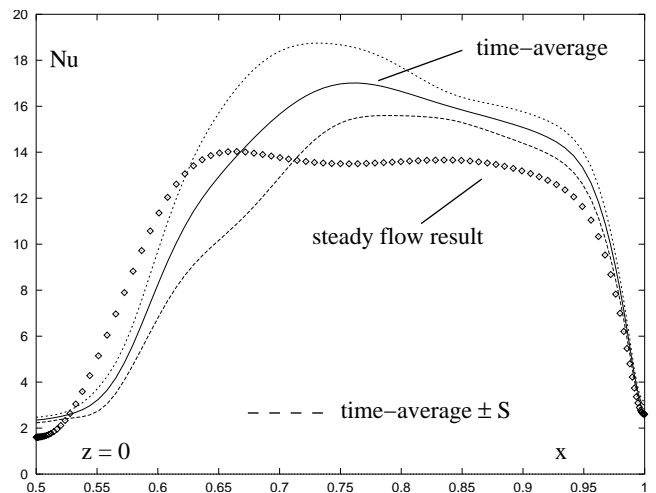


Fig. 4 Nusselt numbers for incompressible flow computations:  $Re_\phi = 10^4$

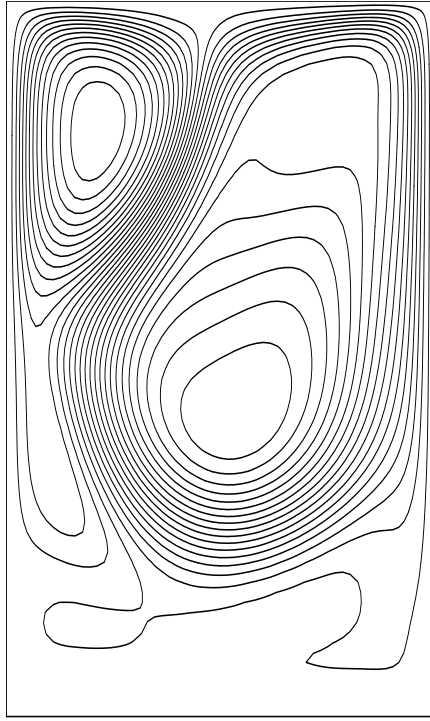


Fig. 5 Steady-state secondary flow streamlines for variable density flow computation:  $Re_\phi = 10^4$

values for  $Nu$  over most of the disc than were computed for steady flow. The standard deviation,  $S$ , of local Nusselt number about the time-averaged distribution (taken over the entire simulation) illustrates that the greatest variation of  $Nu$  with time occurs in the lower part of the cavity, where the radial inflow of air near the mid-plane turns toward one or other of the discs.

#### 4 EFFECTS OF DENSITY VARIATIONS

The unsteady computation described above was repeated with density variations in the flow accounted for, using the Boussinesq approximation, as described in section 2. The conditions  $Re_\phi = 10^4$  and  $\Delta T = 50$  K give a

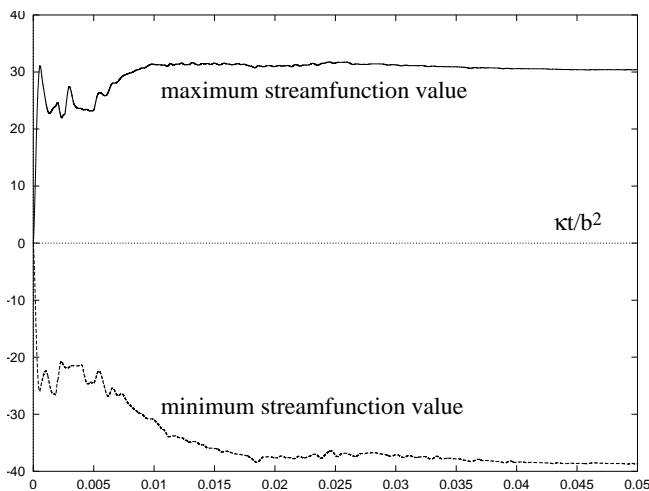


Fig. 6 Streamfunction time-history for unsteady variable density flow computation:  $Re_\phi = 10^4$

Rayleigh number  $Ra \approx 1.1 \times 10^7$  for this problem (the definition of  $Ra$  is given in the nomenclature).

The variable density time-dependent computation developed to a steady flow structure, with asymmetric secondary-flow recirculations, and this is shown in Fig. 5. The radial inflow between the discs is directed toward the heated disc, at dimensionless radius  $x \approx 0.75$ . Fig. 6 illustrates the approach to the steady state in terms of the variation of maximum and minimum values of streamfunction with nondimensional time.

Fig. 7 shows the computed local  $Nu$  distribution for the heated disc for the steady-state solution. The two peaks in Nusselt number correspond to the inner region where recirculating flow is moving toward the disc ( $x \approx 0.6$ ), and the outer region where the radial inflow is turned toward the disc ( $x \approx 0.85$ ). This steady-state result was also compared with computations carried out using the steady elliptic solver from Mirzaee et al (1997). The latter code incorporates variable density effects directly, i.e. the Boussinesq approximation is not used. The code gave the same general solution and distribution for  $Nu$  as shown in Fig. 5 and Fig. 7: the position of the two peaks were radially outward of those shown in Fig. 7, but were of very similar magnitude.

The influence of density variations on the stability of the flow at  $Re_\phi = 10^4$  was studied by carrying out further computations for other values of  $\Delta T$ . It was found that unsteady periodic flow, as described in section 3 but with longer period, developed for  $\Delta T$  values up to 30 K ( $Ra = 6.6 \times 10^6$ ), and that steady-state conditions were reached for  $\Delta T = 40$  K ( $Ra = 8.7 \times 10^6$ ) and above. Similar computations were subsequently carried out for the case  $Re_\phi = 1.46 \times 10^5$ , for which Wilson et al (1997) described isothermal axisymmetric computations which were not periodic. For this case, unsteady non-periodic flow continued to develop for Rayleigh numbers up to  $Ra = 4.2 \times 10^9$ , although density effects caused significant changes to time-averaged Nusselt numbers compared with results assuming incompressible flow. As for the  $Re_\phi = 10^4$  case described above, steady state heat

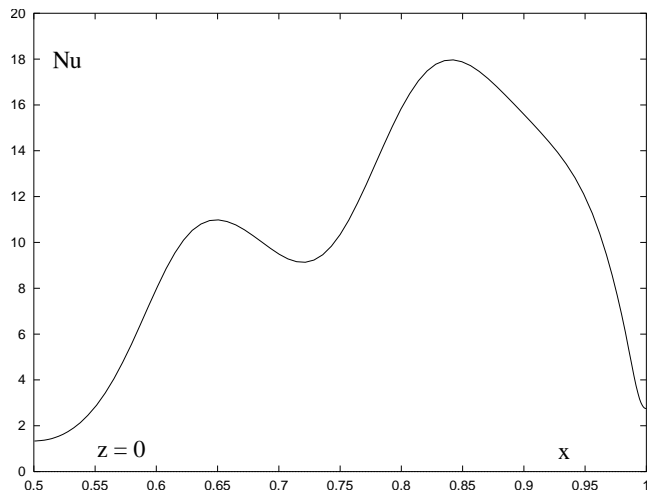


Fig. 7 Steady-state Nusselt numbers for variable density flow computation:  $Re_\phi = 10^4$

transfer computations carried out using a finite-volume solver at  $Re_\phi = 1.46 \times 10^5$  significantly underpredicted time-averaged Nusselt numbers computed for the unsteady flow.

## 5 CONCLUSIONS AND RECOMMENDATIONS

Computational results have been obtained for unsteady axisymmetric laminar flow and heat transfer in a rotating cavity with a stationary outer surface. Computed flow structures and disc surface Nusselt numbers are significantly affected by modelling assumptions such as steady flow and incompressibility. In particular, steady flow solutions underpredict peak Nusselt numbers obtained from unsteady calculations. It is probable that unsteady flow and variable density effects also need to be considered in making comparisons between computational results and existing experimental data for other cases involving turbulent flow.

## NOMENCLATURE

a, b	inner, outer radius of disc
G	gap ratio ( $= s/b$ )
k	turbulent kinetic energy
Nu	Nusselt number ( $= qr/\kappa(T_o - T_s)$ )
Pr	Prandtl number
q	heat flux from heated disc to air
r	radial coordinate
Ra	Rayleigh number ( $= Re_\phi^2 Pr \beta \Delta T$ )
$Re_\phi$	rotational Reynolds number ( $= \rho \Omega b^2 / \mu$ )
s	axial gap between discs
S	standard deviation
t	time
T	temperature
$T_o$	surface temperature of heated disc ( $z = 0$ )
$T_s$	surface temperature of unheated disc ( $z = s$ )
$V_r, V_\phi, V_z$	time-averaged velocities in r, $\phi$ , z directions
x	nondimensional radius ( $= r/b$ )

z	axial coordinate
$\beta$	volumetric expansion coefficient ( $= 2/(T_o + T_s)$ )
$\delta t$	solution time step
$\Delta T$	temperature difference ( $= T_o - T_s$ )
$\epsilon$	turbulent energy dissipation rate
$\kappa$	thermal conductivity
$\mu$	dynamic viscosity
$\rho, \rho_o$	density, reference density
$\phi$	tangential coordinate
$\Omega$	angular speed of discs

## REFERENCES

- Gan, X., Mirzaee, I., Owen, J. M., Rees, D. A. S. and Wilson, M. 1996 Flow in a rotating cavity with a peripheral inlet and outlet of cooling air, ASME Int. Gas Turbine and Aeroengine Cong., Birmingham, paper 96-GT-309
- Launder, B. E. and Sharma, B. I. 1974 Application of the energy dissipation model of turbulence to flow near a spinning disc, Letters in Heat and Mass Transfer, vol 1, 131-138
- Mirzaee, I., Gan, X., Wilson, M. and Owen, J. M. 1997 Heat transfer in a rotating cavity with a peripheral inflow and outflow of cooling air, ASME Int. Gas Turbine and Aeroengine Cong., Orlando, paper 97-GT-136
- Owen, J.M. and Rogers, R.H. 1995, Flow and heat transfer in rotating disc systems: Vol. 2, Rotating cavities [Research Studies Press, Taunton, UK and John Wiley, NY, USA]
- Wilson, M., Arnold, P. D., Lewis, T. W., Mirzaee, I., Rees, D. A. S. and Owen, J. M. 1997 Instability of flow and heat transfer in a rotating cavity with a stationary outer casing, Eurotherm 55 (Heat Transfer in Single Phase Flow), Santorini, Greece, September